Chemical Science

ROYAL SOCIETY OF CHEMISTRY

PERSPECTIVE

View Article Online
View Journal | View Issue

Cite this: *Chem. Sci.*, 2022, **13**, 1883

All publication charges for this article have been paid for by the Royal Society of Chemistry

Received 11th August 2021
Accepted 7th December 2021

DOI: 10.1039/d1sc04413c

rsc.li/chemical-science

Recent advances in upconversion nanoparticle-based nanocomposites for gas therapy

Nailin Yang, Fei Gong and Liang Cheng *

Gas therapy has attracted wide attention for the treatment of various diseases. However, a controlled gas release is highly important for biomedical applications. Upconversion nanoparticles (UCNPs) can precisely convert the long wavelength of light to ultraviolet/visible (UV/Vis) light in gas therapy for the controlled gas release owing to their unique upconversion luminescence (UCL) ability. In this review, we mainly summarized the recent progress of UCNP-based nanocomposites in gas therapy. The gases NO, O_2, H_2, H_2S, SO_2, and CO play an essential role in the physiological and pathological processes. The UCNP-based gas therapy holds great promise in cancer therapy, bacterial therapy, anti-inflammation, neuromodulation, and so on. Furthermore, the limitations and prospects of UCNP-based nanocomposites for gas therapy are also discussed.

1. Introduction

Over the past few decades, upconversion nanoparticles (UCNPs) have attracted wide attention owing to their unique upconversion luminescence (UCL) ability, where two or more low-energy excitation photons (*e.g.*, near-infrared light (NIR)) are converted into shorter wavelength emission/higher-energy photons (*e.g.*, visible (Vis) and ultraviolet (UV)).[1–6] Their superior high quantum yield, chemical stability, and regulable optical properties achieved by altering lanthanide dopants or host substrates make them well-suited for biomedical applications, such as bioimaging,[7–9] biodetection,[10–12] drug delivery,[13] and cancer therapy.[14–16] UCNPs show excellent properties, such as zero auto-fluorescence background, large anti-Stokes shift, narrow emission band, and deeper tissue penetration, for long-term repeated biological imaging. UCNP-based biological imaging using luminescence resonance energy transfer (LRET) shows a better signal-to-noise ratio than traditional biological imaging. UCNP-based imaging involves a wide range of imaging modalities, from single modal imaging to multi-modal imaging in combination with magnetic resonance imaging (MRI), photoacoustic imaging (PA), computerized tomography (CT), and positron emission tomography (PET).[8] Bio-detection mainly uses UCNPs as the energy donors and then selects appropriate energy receptors to realize the detection of target objects using LRET. At present, the biometric probes that use UCNPs have realized the highly sensitive detection of metallic ions (Hg^{2+}, Cr^{3+}, Pb^{2+}, and Ag^{+}) and biomolecules (protein, nucleic acids, and small molecules).[10] Apart from bio-detection and imaging, UCNPs have also shown great promise for therapeutic

Institute of Functional Nano & Soft Materials (FUNSOM), Jiangsu Key Laboratory for Carbon-Based Functional Materials and Devices, Soochow University, Suzhou 215123, China. E-mail: lcheng2@suda.edu.cn

Nailin Yang received his B.S. degree from Qingdao University of Science and Technology in 2018. Since then, he has been pursuing his Ph.D. degree at the Institute of Functional Nano & Soft Materials (FUNSOM) of Soochow University, under the supervision of Prof. Liang Cheng and Prof. Zhuang Liu. His research interest is focused on multi-functional biomaterials for cancer therapy and tissue engineering.

Fei Gong received his B.S. degree from Zhejiang Sci-Tech University in 2016 and Ph.D. degree from Soochow University in 2021. Since then, he worked at the Institute of Functional Nano & Soft Materials (FUNSOM) of the Soochow University as a post-doc. His research interest is focused on multifunctional nanomaterials for cancer theranostics.

applications, especially for cancer treatment.[17–19] Like many other nanomaterials, UCNPs with controllable surface chemistry (*e.g.*, physical adsorption,[13] UCNP@MOF (metal–organic framework) composites,[20] UCNP@SiO_2 (mesoporous silica)) can be used as a drug delivery system (*e.g.*, chemical drugs, targeted groups, and photosensitive molecules). Above all, UCNPs with unique UCL performance are promising for bio-applications.

As a promising therapeutic method, gas therapy has recently attracted much attention in treating various diseases (*e.g.*, cancer, inflammatory, neuromodulation, and cardiovascular diseases).[21–23] The gas therapy involves gases, such as nitric oxide (NO), oxygen (O_2), hydrogen (H_2), hydrogen sulfide (H_2S), sulfur dioxide (SO_2), and carbon monoxide (CO), that play a vital role in the physiological and pathological processes. Due to the beneficial physical and chemical properties of nanomaterials, the gas-generating nanoplatforms could, on the one hand, specifically generate the required therapeutic gases used in personalized treatments,[24–26] and on the other, effectively accumulate in the diseased tissues for improved gas delivery using enhanced permeability and retention (EPR) or by actively targeting the suitable surface modification.[27] Though various nanocarriers have been recently developed for generating gas, the *in vivo* therapeutic application still faces major challenges due to the uncontrollability of these gases. For instance, NO within the concentration range of 10^{-6} to 10^{-3} M yields direct anti-cancer effects; however, higher concentrations (>1 mM) in the blood may potentially cause NO poisoning.[28] Therefore, a controlled gas release is of high importance in medical applications.

Based on the stimulation route, the controllable release stimulation of nanoplatforms can be classified into endogenous and exogenous stimulation triggers. Among the gas-generation strategies, exogenous light-stimulation has attracted a great deal of interest in controlling the spatial and temporal release of the gas, achieving accurate and predictable gas release.[24] The most efficient light-stimulated gas release strategies usually require direct excitation by UV/Vis light. The main advantage of the photochemically triggered gas release of precursors using UV/Vis light is that photoexcitation can provide precise control over the timing, location, and dose of the prodrug. UCNP, due to their unique UCL performance, can precisely convert the long wavelengths of light with strong tissue penetration depth into short wavelengths of light that can induce gas generation. Using the flexibility of photo-stimulation, the dose-dependent biological effects could be achieved and adjusted with a light-controlled gas-releasing nanoplatform. Ideally, the amount of gas should be directly monitored to find the optimum between toxic effects and inefficiency. At present, some quantitative gas detection methods (*e.g.*, gas chromatography, Griess assay, and gas microelectrode), can be used to monitor the gas concentration in tissues in real-time, and thus can control the power and distance of the excited light.[23,24,29] Therefore, the development and application of UCNP-based nanocomposites to realize the controlled release of therapeutic gases are greatly desired. However, there is no systematic summary of UCNP-based gas therapies to guide bio-application in the literature. The current review summarizes the recent progress of the gas therapy of UCNP-based nanocomposites. These gases (NO, O_2, H_2, H_2S, SO_2, and CO) are therapeutic and play a vital role in the physiological and pathological processes. Gas therapy using UCNP-based nanocomposites holds great promise for bio-application, such as in cancer therapy, anti-inflammatory therapy, and neuromodulation (Scheme 1). The advantages and necessity of UCNP-based gas therapy are systematically summarized, and the prospects and opportunities for the therapy are also discussed. This concise yet comprehensive review might stimulate and guide further in-depth studies on UCNP-based nanocomposites in gas therapy.

Dr Liang Cheng received his Ph.D. degree from the Institute of Functional Nano & Soft Materials (FUNSOM) at Soochow University in 2012, and then joined Soochow University as a faculty member. He was promoted to an associate professor in 2014 and a full professor in 2018. His research work has been focused on the development of multifunctional nanomaterials for biomedical application. He is currently serving as an associate editor for Journal of Nanobiotechnology.

2. Mechanisms of UCNPs luminescence and energy transfer

Upconversion luminescence (UCL) is a nonlinear optical process. During this process, UCNPs are excited by multiple low-energy photons (*e.g.*, NIR with a long wavelength), and emit a high-energy photon (*e.g.*, UV/Vis with a shorter wavelength).[1,30] This phenomenon is mainly because their orbital arrangement of $4f^n$ (n: 0–14) can provide various electronic properties. In a word, The UCL process mainly depends on the ladder-like arrangement of energy levels of doped rare-earth ions. Essentially, a UCNP shall be doped by two different ions, one of them is an activator (luminescent center), and the other is a sensitizer. In addition, the crystal structure and optical properties of matrix (host materials) also play a pivotal role in realizing efficient UCL processes. Excited energies of the activated ions may be absorbed by the matrix through lattice vibration. Different crystal structures of the host materials would also lead to the variation of the crystal field around the activated ions, resulting in different optical properties of the nanoparticles. Indeed, the mechanism of the absorption consists of five parts, which might be involved in this process either alone or in combination: excited state absorption (ESA), cooperative sensitization upconversion (CSU), cross relaxation (CR), energy transfer upconversion (ETU), and photon avalanche (PA).[1] The ETU route is of practical importance for UCNPs investigation, since the most effective UCNPs to date have exploited this approach for enhanced excitation and efficient upconverted emissions.

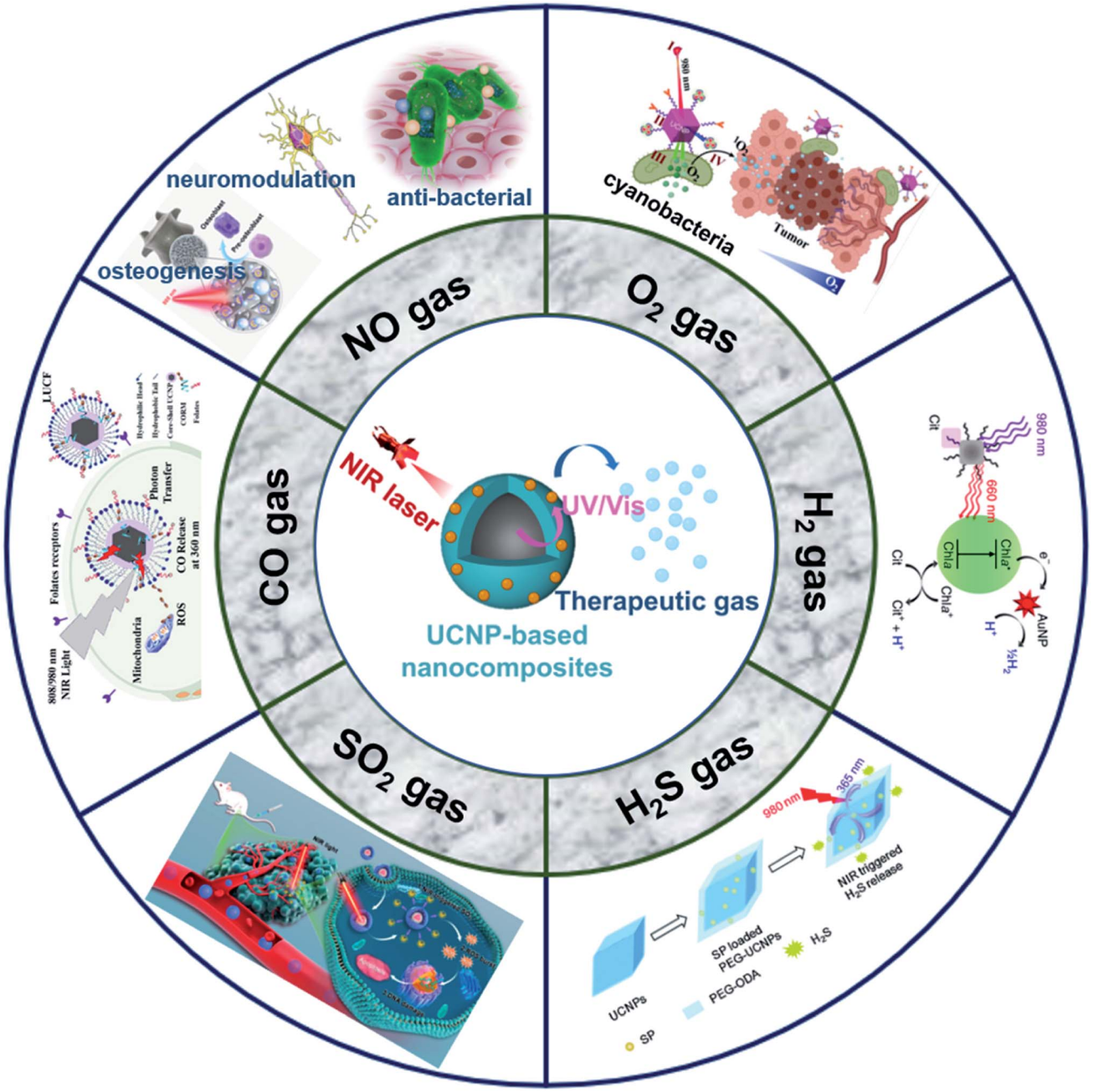

Scheme 1 Schematic illustration shows the application of the UCNP-based nanocomposites for gas therapy. NO,[29,54,57] O_2,[84] H_2,[42] H_2S,[38] SO_2,[39] and CO.[100] Adapted from ref. 29 with permission from American Association for the Advancement of Science, copyright 2020; adapted from ref. 54 with permission from Elsevier Ltd, copyright 2021; adapted from ref. 57 with permission from American Chemical Society, copyright 2021; adapted from ref. 84 with permission from Springer, copyright 2021; adapted from ref. 42 with permission from Nature Publishing Group, copyright 2020; adapted from ref. 38 with permission from Royal Society of Chemistry, copyright 2015; adapted from ref. 39 with permission from American Chemical Society, copyright 2019; adapted from ref. 100 with permission from Elsevier Ltd, copyright 2019.

LRET is a radiative process where light emitted by a donor is absorbed by acceptor molecules. Lanthanide-doped UCNPs (Ln-UCNPs) that exploited the ETU pathways, containing three components, namely a sensitizer (*e.g.*, Yb^{3+}, Nd^{3+}), an emitter (*e.g.*, Er^{3+}, Tm^{3+}, Ho^{3+}), and a host matrix (*e.g.*, fluoride), can be excited with deep-tissue penetrating NIR light (*e.g.*, 980 nm) and emit light in a range from UV to NIR. Efficient Ln-UCNPs require reasonable adjustment between host matrix, doping ions, and dopant concentration. Yb^{3+} and Nd^{3+} ions are the most widely used sensitizers in UCNPs that are activated by 980 nm and 800 nm laser, respectively, due to their larger cross section absorption around the NIR region than that of other lanthanides. In general, the Yb^{3+}/Tm^{3+} system yields UC emissions in the high energy (*e.g.*, blue to UV spectral region), have been reported as promising candidates for the UC process. Since matching energy levels are required, the most

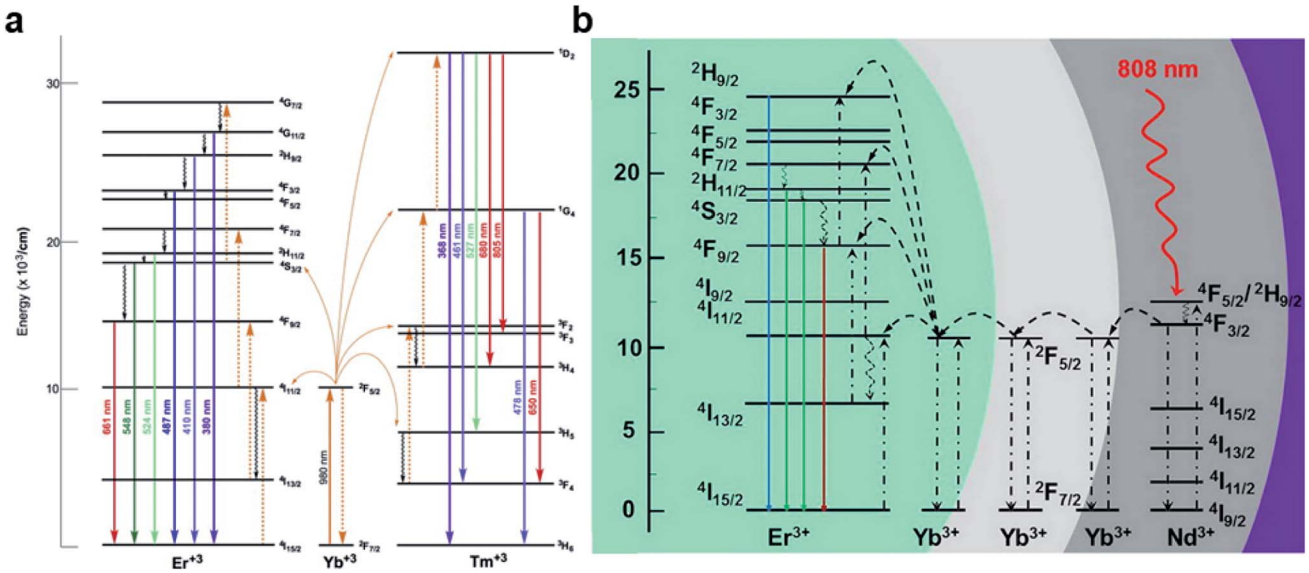

Fig. 1 Proposed energy transfer mechanism showing the UCL processes in (a) Er^{3+}, Tm^{3+}, and Yb^{3+} doped UCNPs under 980 nm laser excitation[31] and (b) Nd^{3+}, Yb^{3+}, and Er^{3+} doped UCNPs under 808 nm laser excitation.[32] Adapted from ref. 31 with permission from Elsevier Ltd, copyright 2014; adapted from ref. 32 with permission from American Chemical Society, copyright 2016.

investigated UCNPs with NaYF4:Yb^{3+}/Er^{3+}(Tm^{3+}) structure, and also efficient Nd^{3+}-sensitized UCNPs which provide a wide range of UV/Vis spectrum under NIR excitation (Fig. 1).[31,32] Since most light-responsive gas donors are responsible to UV/Vis light for direct gas release, UCNP could be used to construct UCNP-based nanocomposites for gas therapy.

3. UCNP-based nanocomposites for gas therapy

Light-controlled gas generation for therapeutic applications has attracted much attention due to its noninvasiveness and practicability. Among light-responsive gas donors, most of them are responsible to UV/Vis light for direct gas release (Table 1). For NO donors, S–NO bonds in S-nitrosothiols (RSNOs),[33] N–NO bond in N-nitrosamines,[34] and O–NO bond in nitrobenzene could be broken for NO release upon UV/Vis light irradiation.[35] Metal–NO complexes, such as Roussin's black salt (RBS, $[Fe_4S_3(NO)_7]^-$), $d_\pi(M)$–$\pi^*(NO)$ transitions could be generated NO under UV/Vis light irradiation. BNN6 (*N*,*N*′-di-*sec*-butyl-*N*,*N*′-dinitroso-1,4-phenylenediamine) can also be activated by UV/Vis light to remove the nitrosyl groups and release NO.[28,36] For CO donors, metal carbonyls (*e.g.*, MnCO, RuCO, *etc.*) are stabilized by the coordination attraction between carbonyls and transition metals, thus are sensitive to UV/Vis light for photochemical degradation into CO.[37] As a H_2S donor, propane-2,2-diylbis((1-(4,5-dimethoxy-2-nitrophenyl)ethyl)sulfane) (SP), is easily cracked into gem-dithiols by UV light, and unstable gem-dithiols are readily hydrolyzed to release H_2S gas.[38] As a closed-ring isomer of a diarylethene, 1-(2,5-dimethylthien-1,1-dioxide-3-yl)-2-(2,5-dimethylthien-3-yl)-hexafluorocyclopentene (DM) molecule can generate SO_2 gas rapidly by reverting to the open-ring isomer upon UV light irradiation.[39] However, most of them are only sensitive to UV/Vis light, and the penetration depth of UV/Vis light greatly limits their application in living organisms. By contrast, using NIR light as the light stimulation source would undoubtedly be a better choice due to its higher tissue penetration ability.[40,41]

UCL ability of UCNPs can cleverly activate these photosensitive gas molecules, significantly expanding its potential bioapplications. Although few photosensitive gas molecules can produce O_2 or H_2 gas, the UCL ability of UCNP could still play a vital role in constructing UCNP-based nanocomposites to realize O_2 therapy (*e.g.*, O_2-enhanced photodynamic therapy) or H_2 therapy (*e.g.*, anti-inflammatory).[42,43]

3.1 UCNP-based NO gas therapy

NO is an important signaling molecule that transits biochemical signals, and plays a vital role in various physiological and pathological processes such as cancer therapy, antimicrobial therapy, immune regulation, angiogenesis, and neuromodulation.[44–47] Several studies have shown that the low concentrations of NO gas promote tumor growth, while the relatively high concentrations induce an anti-tumor effect by inhibiting cell respiration. Zhang *et al.* demonstrated that UCNPs trigger NO release from NO precursor Roussin's black salt (RBS) when irradiated by a 980 nm laser (Fig. 2a).[48] RBS loaded into mesoporous silica (SiO_2) on the surface of UCNP led to LRET between UCNP and RBS, which triggered the photoreaction of RBS and the release of NO. Such nanocomposites showed great inspirations for the photo-stimulated delivery of bioactive molecules for imaging and cancer therapy. Later, Zhao *et al.* demonstrated a similar strategy by using SiO_2 adsorbed RBS onto UCNPs for cancer treatment.[49] By regulating the NIR laser power density, the on-demand and dose-controllable release of NO was achieved (Fig. 2b). In addition, NO could be

Table 1 Summary of light-responsive molecules and the chemical route of gas release

Gas classification	Prodrug/catalyst	Molecular structures	Excitation wavelength	Chemical route of gas release	Ref.
NO	S-Nitrosothiols (RSNO)	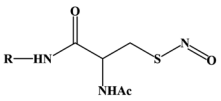	UV/Vis	S–NO bonds were broken	34
	N-Nitrosamines	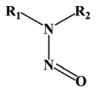		N–NO bond were broken	34
	Nitrobenzene	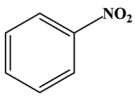		O–NO bond were broken	35
	Metal–NO complexes, such as Roussin's black salt (RBS, $[Fe_4S_3(NO)_7]^-$)	—		Metal-NO bond were broken 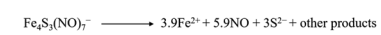	48
	BNN6 (*N*,*N*′-di-*sec*-butyl-*N*,*N*′-dinitroso-1,4-phenylenediamine)	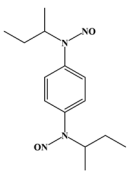		Nitrosyl groups were removed 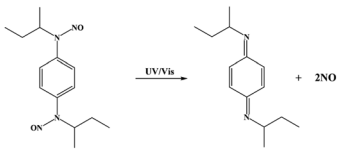	36
O_2	MnO_2	—	—	Catalase-like enzyme	72
	$Fe(OH)_3$	—			79
	CeO_2	—			43 and 83
	Cyanobacteria	—	Vis (660 nm)	Photosynthesis	84
H_2	Chlorophyll a (Chla) + AuNPs	—	Vis (660 nm)	Photocatalytic H_2 evolution	42
CO	Metal carbonyls	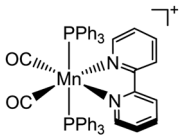	UV (360 nm)	M-NO bonds were broken 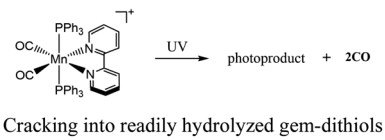	37
H_2S	Propane-2,2-diylbis((1-(4,5-dimethoxy-2-nitrophenyl) ethyl)sulfane) (SP)	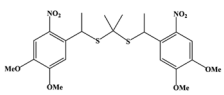	UV (365 nm)	Cracking into readily hydrolyzed gem-dithiols 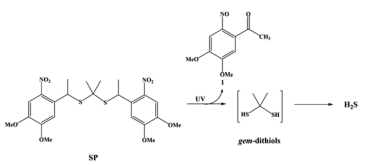	38
SO_2	1-(2,5-Dimethylthien-1,1-dioxide-3-yl)-2-(2,5-dimethylthien-3-yl)-hexafluorocyclopentene (DM)	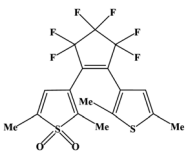	UV (365 nm)	Reverting to the open-ring isomer 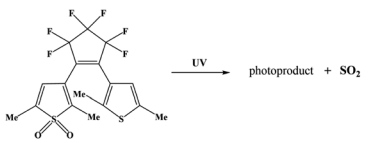	39 and 97

used as an adjuvant drug to enhance diagnosis and treatment. For example, NO sensitized the multidrug-resistant cancer cells to the drugs, thus, greatly enhancing chemotherapy efficacy. The strong power density irradiation accompanied by a high concentration of NO effectively inhibited tumor growth. On the other hand, low-dose NO generated by the weak power irradiation inhibited the P-glycoprotein (P-gp) expression on the membrane in drug-resistant tumor cells, and thus, sensitized the multidrug-resistant cells to improve the effectiveness of chemotherapy. Recently, a similar nanoplatform was developed using Ca^{2+}-doped UCNP@SiO_2 loaded with a ruthenium nitrosyl complex [(3)Ru(NO)(Cl)] to realize enhanced fluorescence intensity to trigger the release of NO when irradiated by NIR light (Fig. 2c).[50] After Ca^{2+} doping, the nanocomposites exhibited ~300 times higher UCL intensity than the bare-UCNPs. The Ca-doped UCNPs showed no obvious toxicity to cancer cells without the 980 nm laser irradiation, while the toxic NO gas was readily generated to kill cancer cells after 980 nm laser irradiation. Additionally, a UCNP-based all-in-one multifunctional nano-theranostic platform was designed for UCL/MRI/CT

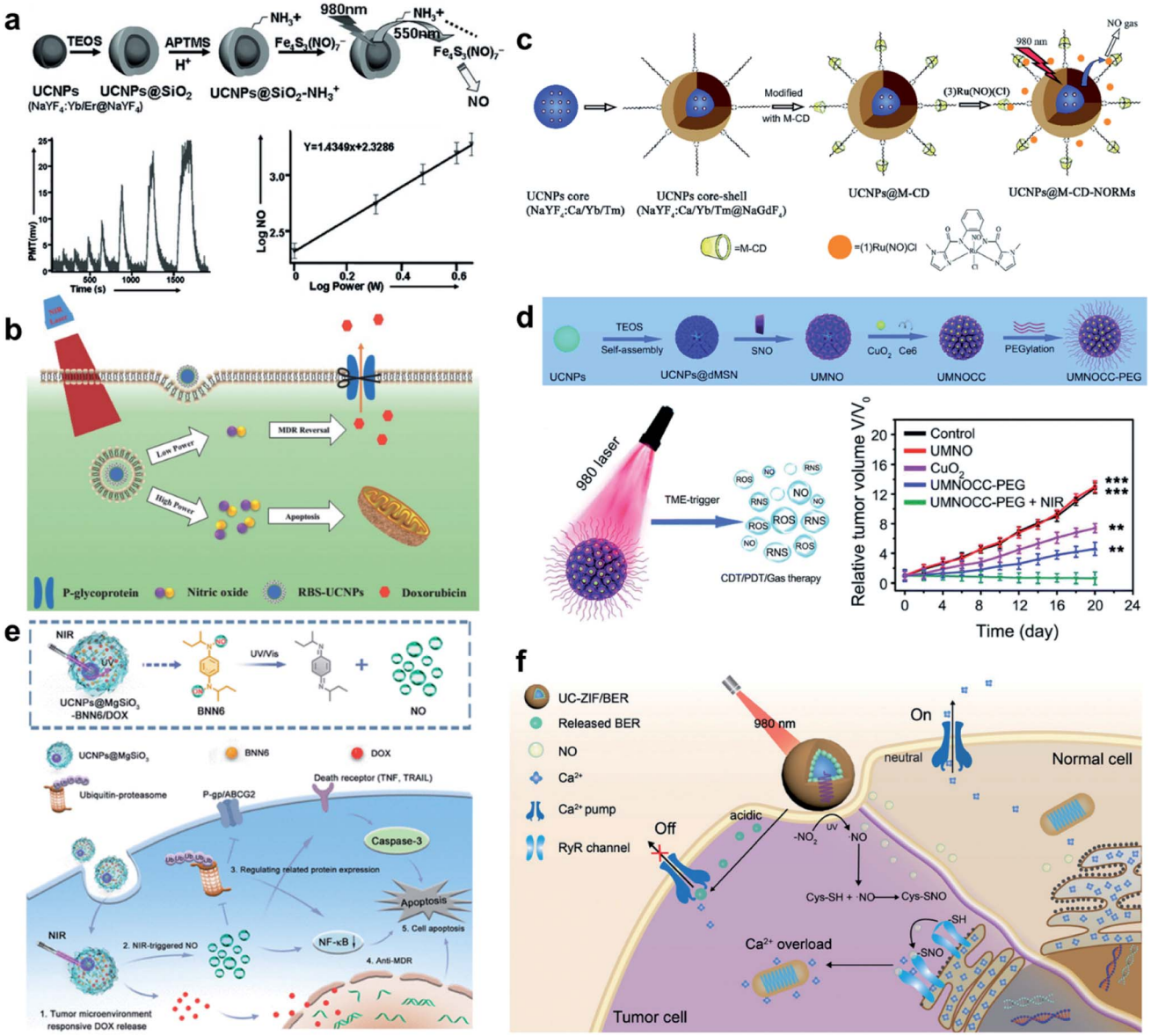

Fig. 2 UCNP-based nanocomposites for NO gas cancer therapy. (a) Synthesis of the UPNPs@SiO_2@RBS nanostructures for NIR light triggered photochemical NO release.[48] (b) NIR light-triggered on-demand NO release for dose-dependent tumor therapy.[49] (c) Enhanced luminescence intensity of near-infrared sensitized UCNP-based nanocomposites *via* Ca^{2+} doping for NO release.[50] (d) An all-in-one theranostic nanoplatform based on UCNP-based nanocomposites for synergistic CDT/PDT/gas therapy.[51] (e) Light-switchable yolk-mesoporous shell UCNPs@$MgSiO_3$ for NO-evoked multidrug resistance reversal in cancer therapy.[52] (f) Intracellular calcium stores modulated by NO for Ca^{2+}-initiated cancer therapy.[53] Adapted from ref. 48 with permission from Wiley-VCH, copyright 2012; adapted from ref. 49 with permission from Wiley-VCH, copyright 2015; adapted from ref. 50 with permission from Royal Society of Chemistry, copyright 2020; adapted from ref. 51 with permission from Royal Society of Chemistry, copyright 2020; adapted from ref. 52 with permission from American Chemical Society, copyright 2020; adapted from ref. 53 with permission from Wiley-VCH, copyright 2021.

trimodal bioimaging-guided synergistic chemodynamic therapy (CDT)/PDT/gas therapy (Fig. 2d).[51] In this nanoplatform, UCNPs@SiO_2 were prepared for loading NO donor. Subsequently, the copper peroxide nanodots (CuO_2), chlorin e6 (Ce6), and polyethylene glycol (PEG) were loaded into SiO_2 pores to obtain UCNP-based multifunctional nanocomposites (UCNP@SiO_2–SNO@CuO_2–Ce6-PEG). Multimodal imaging was achieved using CT imaging performance of Yb and Gd elements (high atomic number), MRI imaging properties of the Gd element (T_1 signal), and strong green UCL images of Er element. Furthermore, the copper ions accelerated the NO release, thereby, achieving synergistic CDT/PDT/gas therapy when irradiated by NIR laser. A NIR light-switchable NO delivery nanoplatform based on a yolk–shell UCNP@magnesium silica (UCNP@$MgSiO_3$) was designed to achieve the combination therapy of NO and doxorubicin (DOX) (Fig. 2e).[52] The unravel molecular mechanisms was also proved, which inhibited ubiquitin-proteasome and NF-κB signaling pathways. This

UCNP-based nanoplatform developed a promising combination therapy of gas therapy and chemotherapy. Recently, a UCNP-based Ca^{2+} store regulating system was developed by UCNP@-MOF loaded with berbamine (Fig. 2f).[53] The diffused NO invaded the overexpressed RyRs for protein S-nitrosylation, opening the RyRs and allowing Ca^{2+} to flow out of the endoplasmic reticulum. Meanwhile, berbamine, as a calcium pump inhibitor, could inhibit Ca excretion to maintain high Ca^{2+} content. This work provides the idea of ion-interference therapy by regulating endogenous Ca for cells apoptosis based on UCNP nanocomposites.

In addition to cancer therapy, UCNP-based NO therapy is also investigated for other applications, such as antibacterial, tissues/nerve protection, and regeneration.[54–56] NO shows broad-spectrum anti-bacterial activity while avoiding antimicrobial resistance, and it has aroused wide interests in the treatment of various bacterial infections. For example, a UCNP-based nanocomposite membrane was developed for NO-assisted PDT anti-bacterial treatment under NIR irradiation (Fig. 3a).[54] UCNP@MOF loaded with L-arginine (LA) were encapsulated into polyvinylidene fluoride (PVDF) membrane. Under NIR irradiation, the UCNP membrane could generate sufficient reactive oxygen species (ROS) and further induce NO generation, thus realizing the NO/PDT anti-bacterial therapy. Moreover, NO can effectively promote the proliferation and differentiation of osteoblasts. Recently, bone-targeted UCNP-based nanocomposites were designed and synthesized as the NIR-responsive gas nanoplatform, for targeting the controllable NO release by adjusting the output power of the NIR laser irradiation, osteoblast differentiation in bone tissue and

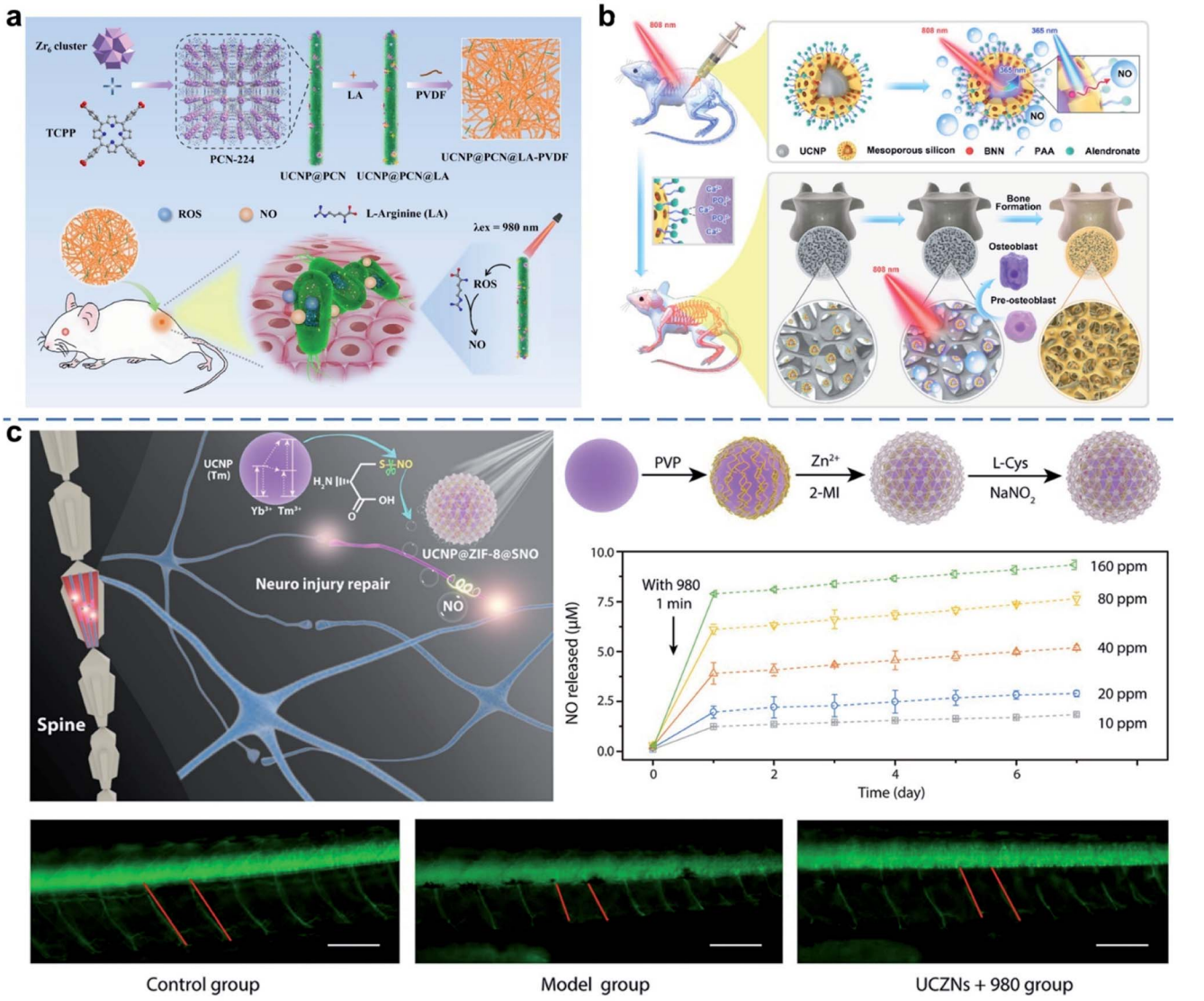

Fig. 3 UCNP-based nanocomposites for NO gas therapy of tissues/nerve protection and regeneration. (a) NIR-triggered PDT and NO synergistic anti-bacterial nanocomposite membrane.[54] (b) NIR and UCNP defined NO-based osteoporosis targeting therapy.[57] (c) NIR-controlled NO release for SCI repair.[29] Adapted from ref. 54 with permission from Elsevier Ltd, copyright 2021; adapted from ref. 57 with permission from American Chemical Society, copyright 2021; adapted from ref. 29 with permission from American Association for the Advancement of Science, copyright 2020.

reversing osteoporosis was achieved (Fig. 3b).[57] Traumatic spinal cord injury (SCI) is a neurological disease caused by an external physical shock.[58,59] In traumatic SCI, the long axons of the spinal cord neurons are usually severed, which causes a complex cascade of cellular and molecular events including nerve damage and death. NO acts as a messenger for initiating nerve regeneration to protect against inflammation and apoptosis. Bu *et al.* constructed a UCNP-based multi-effect messenger strategy to achieve an on-demand controlled release of NO and alleviate SCI by employing nerve regeneration and neuroprotection (Fig. 3c).[29] This functional nanoplatform was designed with UCNPs coated with zeolitic imidazolate framework-8 (ZIF-8), which could load NO donor nitrosothiol (CysNO) by the large pore size and pore surface area. The UCL ability of UCNPs breaks the S–NO bonds of CysNO to release NO after irradiation with NIR light, followed by a slow increase in

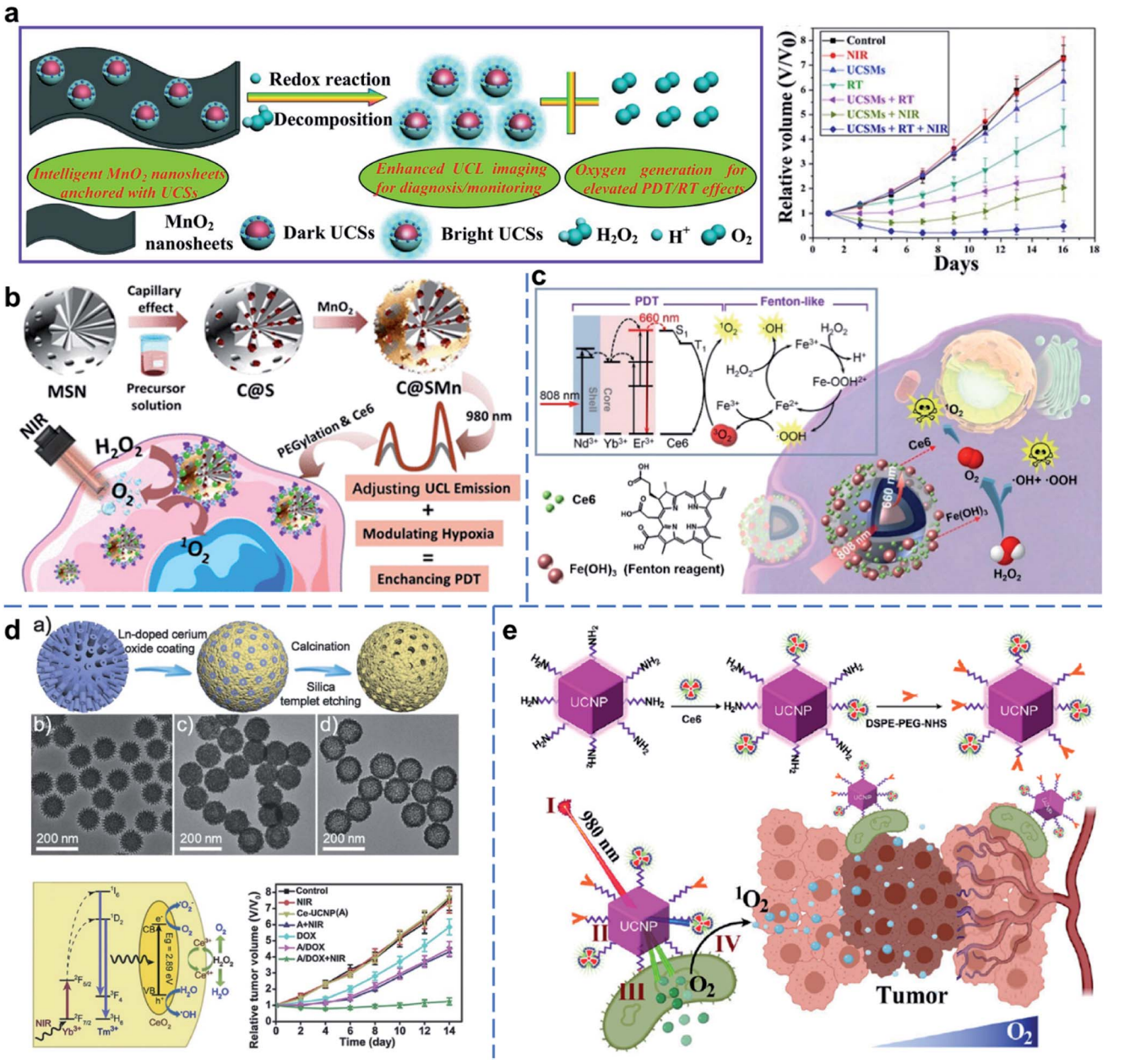

Fig. 4 UCNP-based nanocomposites for O_2 gas therapy. (a) Intelligent MnO_2 nanosheets anchored with UCNPs for concurrent pH-/H_2O_2-responsive UCL imaging and O_2-elevated synergetic therapy.[72] (b) UCNP-based nanocomposites for tumor hypoxia modulation and enhanced photodynamic therapy.[78] (c) Ferric hydroxide-modified UCNPs for NIR-triggered synergetic tumor therapy with hypoxia modulation.[79] (d) CeO_2-modified UCNPs for concurrent pH-/H_2O_2-responsive O_2-evolving synergetic cancer therapy.[83] (e) Cyanobacteria-based NIR-excited self-supplying O_2 system for enhanced photodynamic therapy of hypoxic tumors.[84] Adapted from ref. 72 with permission from Wiley-VCH, copyright 2015; adapted from ref. 78 with permission from American Chemical Society, copyright 2018; adapted from ref. 79 with permission from American Chemical Society, copyright 2018; adapted from ref. 83 with permission from Wiley-VCH, copyright 2018; adapted from ref. 84 with permission from Springer, copyright 2021.

NO level. The dorsal root ganglion (DRG) neurons momentarily fluoresced when locally irradiated with NIR, which meant that the release of NO activated the differentiation pathway for neuronal growth processes. *In vivo* experiments showed that NO treatment induced using this strategy significantly facilitated the repair of the damaged axons of zebrafish motor neurons and promoted motor rehabilitation in rats with traumatic SCI. This strategy widened the applicability of UCNP-based gas therapy in neurological research.

In short, the controlled on-demand NO release by UCNP-based nanocomposites not only plays an essential role in cancer therapy, but also in nerve repair and in other pathological processes. Moreover, the mechanism of NO gas therapy is relatively clear, and UCNP-based nanocomposites can be used to treat various diseases through NO gas therapy. Distinct from H_2S and CO, NO has a longer history of study on its physiological roles and tumor treatment prospect. However, intelligent NO donors that are naturally stable and only release gas under exogenous or endogenous triggers, are still needed. NO gas therapy is a new research frontier and deserves further exploration.

3.2 UCNP-based O_2 gas therapy

As the second abundant gas in the air, O_2 plays an indispensable role in respiration in animals. In addition, O_2 also plays a vital role in the treatment of diseases. For example, the hypoxic environment is one of the most representative microenvironment features in advanced solid tumors, usually caused by excessive O_2 consumption by the rapidly proliferating cancer cells and abnormal vascular systems.[60,61] In particular, hypoxia may significantly hamper the cancer therapies, such as RT,[62,63] chemotherapy,[64,65] PDT,[66,67] and sonodynamic therapy (SDT).[68,69] Therefore, efficient O_2 generation and delivery strategies have been extensively explored and developed to overcome the hypoxic environment and improve the efficacy of cancer therapies. In addition, ROS-mediated tumor treatment showed better prospects than thermal ablation.[70,71] To address the limited PDT effect, a series of UCNP-based nanoreactors were constructed to improve its therapeutic effects. Typically, an intelligent 2D multifunctional nanoreactor using MnO_2 nanosheets loaded with UCNPs was developed to achieve O_2-enhanced synergetic RT/PDT (Fig. 4a).[72] Owing to the increased proliferation rate of the tumor tissues compared to the normal tissues, the concentration of hydrogen peroxide (H_2O_2) in the tumor microenvironment (TME) is higher than that of the normal tissues.[73–75] Interestingly, H_2O_2 is an endogenous resource that can be catalyzed to generate O_2 using catalase or other catalase-like enzymes. In this nanoreactor, MnO_2 played a crucial role as an effective catalase-like enzyme that reacted with endogenous H_2O_2 to generate O_2 through the classical disproportionation reaction.[76,77] Under NIR/X-ray irradiation, UCNP-based nanoplatform released O_2 to alleviate the hypoxic environment, thereby achieving O_2-dependent synergetic RT/PDT of tumors. Subsequently, a novel UCNP-based O_2-enhanced PDT nanoplatform was constructed using SiO_2 nanospheres with UCNP *in situ* growth inside the pores, then further coated with a thin layer of MnO_2 and loaded with Ce6 photosensitizers (Fig. 4b).[78] These UCNP-based nanocomposites ameliorated tumor hypoxia by triggering the decomposition of H_2O_2 when irradiated with NIR laser, further promoting the therapeutic efficacy of PDT.

In addition, $Fe(OH)_3$ nanomaterials were also proved to be a kind of nano-enzyme that could induce O_2 generation in the presence of H_2O_2. The generation of O_2 was accompanied by the production of ROS through the Fe^{3+}/Fe^{2+} cycle. Therefore, UCNP nanoreactors loaded with Ce6 and, then, coated with $Fe(OH)_3$ were constructed for CDT/PDT synergistic therapy (Fig. 4c).[79] After culturing the cancer cells with UCNP–Ce6–$Fe(OH)_3$ nanoreactors, the presence of H_2O_2 or irradiation by NIR increased intracellular ROS. Above all, UCNP–Ce6–$Fe(OH)_3$ multifunctional nanostructures showed the strongest anti-tumor effect upon irradiation with NIR light. Moreover, cerium oxide (CeO_2) nanoparticles have attracted much attention due to their various enzyme-mimetic properties.[80–82] They can be used as catalase with the ability to transform from Ce^{4+} to Ce^{3+} reversibly, and simultaneously convert H_2O_2 to O_2 and H_2O.[43] Based on this, a novel hollow up-conversion CeO_2 (Ce-UCNP) loaded with chemotherapeutic drug DOX was synthesized to realize highly effective synergetic PDT/chemotherapy (Fig. 4d).[83] After endocytosis of the DOX-loaded Ce-UCNP nanocomposites by cancer cells, DOX was released and O_2 was generated by catalyzing the endogenous H_2O_2, thereby, achieving efficient O_2-evolving synergetic PDT/chemotherapy when irradiated with a 980 nm laser. In addition to catalase-like enzyme mentioned above, cyanobacteria, single-celled prokaryotes that perform O_2-producing photosynthesis, can utilize water as an electron donor to reduce CO_2 into organic carbon compounds along with continuously O_2 releasing under sunlight. Inspired by this, cyanobacteria could be utilized as a living carrier to provide O_2 to improve PDT efficacy, continuously. Recently, a NIR-responsive UCNP@Ce6-cyanobacteria complex was designed and synthesized for effective PDT (Fig. 4e).[84] When irradiated with 980 nm laser, UCNP convert NIR into visible and 660 nm light that could be absorbed by cyanobacteria and Ce6, respectively. Cyanobacteria produced abundant O_2 that could be utilized by Ce6 to generate more ROS to greatly inhibit hypoxic tumor growth.

In short, a series of responsive O_2-producing UCNP nanoreactors were designed to enhance PDT or combination therapy for the characteristics of hypoxia-induced solid tumors. In addition to cancer therapy, diabetes is another common disease that is difficult to treat, and it is often associated with the occurrence and recurrence of diabetic chronic wounds.[85] Improving the local dissolved O_2 is one of the most effective methods to promote the healing of diabetic wounds.[86,87] Therefore, generating the O_2 at the lesion shows important significance for improving the therapeutic effect of these diseases, and exploration of the similar strategy of UCNP-based nanocomposites shows great application prospects in other related diseases (*e.g.*, diabetic chronic wounds). Such UCNP-based O_2 gas therapy strategies could improve the anticancer PDT efficiency, but these proposed treatment methods are still in their infancy, with some potential problems that need to be evaluated in detail, such as how to properly penetrate the

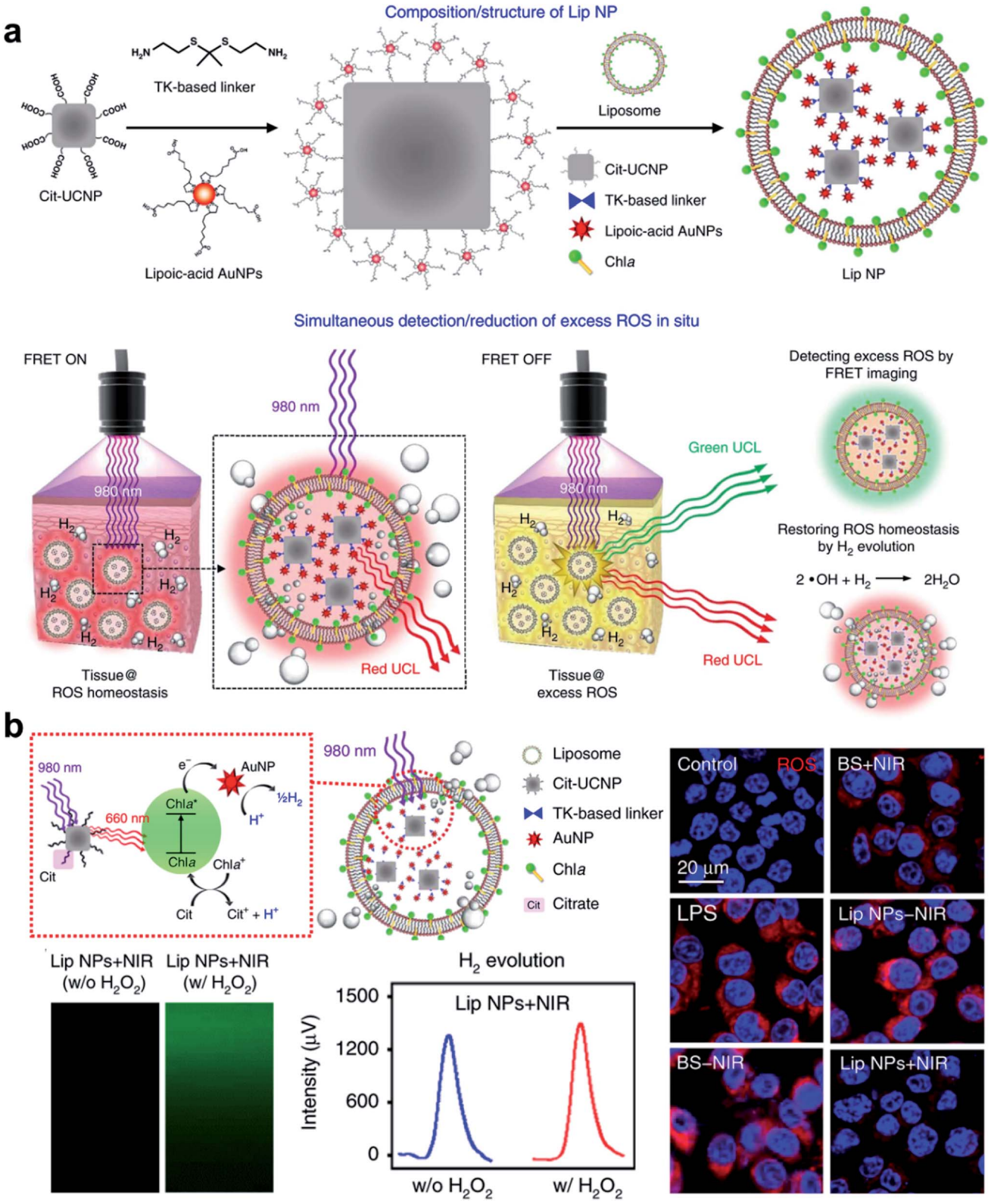

Fig. 5 UCNP-based nanocomposites for H_2 gas therapy. (a) Photosynthesis-inspired H_2 generation using a chlorophyll-loaded liposomal UCNP-based nanoplatform to (b) detect and scavenge excess ROS.[42] Adapted from ref. 42 with permission from Nature Publishing Group, copyright 2020.

hypoxic environment, how to ensure the biosafety and biodegradability of nanocomposites, and *etc.*

3.3 UCNP-based H_2 gas therapy

H_2 is considered a green and safe gas with no potential risk of blood poisoning even at a high concentration. H_2 gas therapy was first used for the treatment of skin squamous cell carcinoma in 1975.[88] Since then, H_2 therapy has received much attention for the treatment of cancer and other inflammatory diseases.[89–91] The use of H_2-rich water and saline has been tested in more than 50 clinical trials on several oxidative stress-related/inflammatory diseases, including type II diabetes mellitus, stroke, Parkinson's disease, and cancer.[92–94] However, it is inconvenient to accurately control gas delivery to the diseased areas with macroscopic administration. Therefore, realizing targeted and controlled H_2 release is essential to augment the curative effect. Recently, UCNP-based nanocomposites were designed and constructed to be applied as a remotely controlled nanoreactor for *in situ* local H_2 generation and eliminate ROS from the diseased cells (Fig. 5a).[42] As a reductive gas, H_2 possesses oxidation resistance for ROS (*e.g.*, $^{\bullet}OH$ and $ONOO^{-}$) scavenging.[94] The nanoreactor consisted of a liposomal system encapsulated with UCNPs, gold nanoparticles (AuNPs) were then bound on the surface of the UCNPs *via* a ROS-responsive thioketal (TK)-based linker, and the lipid bilayer was inserted with chlorophyll a (Chla). The UCNPs functioned as transducers to convert NIR light, which had a deeper penetration depth, into UV light for *in situ* detection and therapy. AuNPs were applied to detect the local ROS, and H_2 was generated by the reaction of protons from citrate (an electron donor) and electrons (photocatalytic electrons) to scavenge the local excess ROS. Notably, after treatment with UCNP-based H_2-generating nanoreactors upon NIR irradiation, the overproduced ROS of macrophages *via* lipopolysaccharide (LPS)-stimulation was greatly reduced (Fig. 5b). In addition, the nanoreactor showed an excellent ability of H_2 generation in environments with either high or normal ROS expression. In addition to ROS elimination, this UCNP-based H_2 generation strategy may also have potential applications in cancer therapy, such as synergistic H_2/PDT therapy.[95] Since H_2 showed anti-tumor activity, an H_2-containing nanosystem (PCN-224@Pd/H_2) was constructed to achieve the synergistic H_2/PDT, which enhanced the anti-tumor effect compared to the singular cancer therapy.

In addition to anti-inflammation, several studies in recent years have shown that H_2 can inhibit tumor growth. Based on the known anti-inflammatory and antioxidant abilities of H_2, it is speculated that H_2 inhibits tumor growth by disrupting the redox status of the tumor microenvironment, activating the caspase-independent apoptosis pathway, and reducing lipid oxidation.[94] However, the antitumor effect of H_2 needs further investigation.

3.4 UCNP-based H_2S gas therapy

H_2S, as an endogenous gaseous transmitter similar to NO, regulates several key biological functions. H_2S induces cytoprotection and anti-inflammatory effects at relatively lower concentrations, and leads to mitochondrial inhibition and cell death (activation of caspase 9 and apoptosis 161) at higher concentrations.[22,40,96] A simple NIR light-induced H_2S generation nanoplatform based on UCNPs was constructed (Fig. 6a).[38] As an H_2S donor, propane-2,2-diylbis((1-(4,5-dimethoxy-2-nitrophenyl)ethyl)sulfane (SP) is easily cracked into gem-dithiols by UV light, and unstable gem-dithiols are readily hydrolyzed to release H_2S. SP was loaded onto the surface of

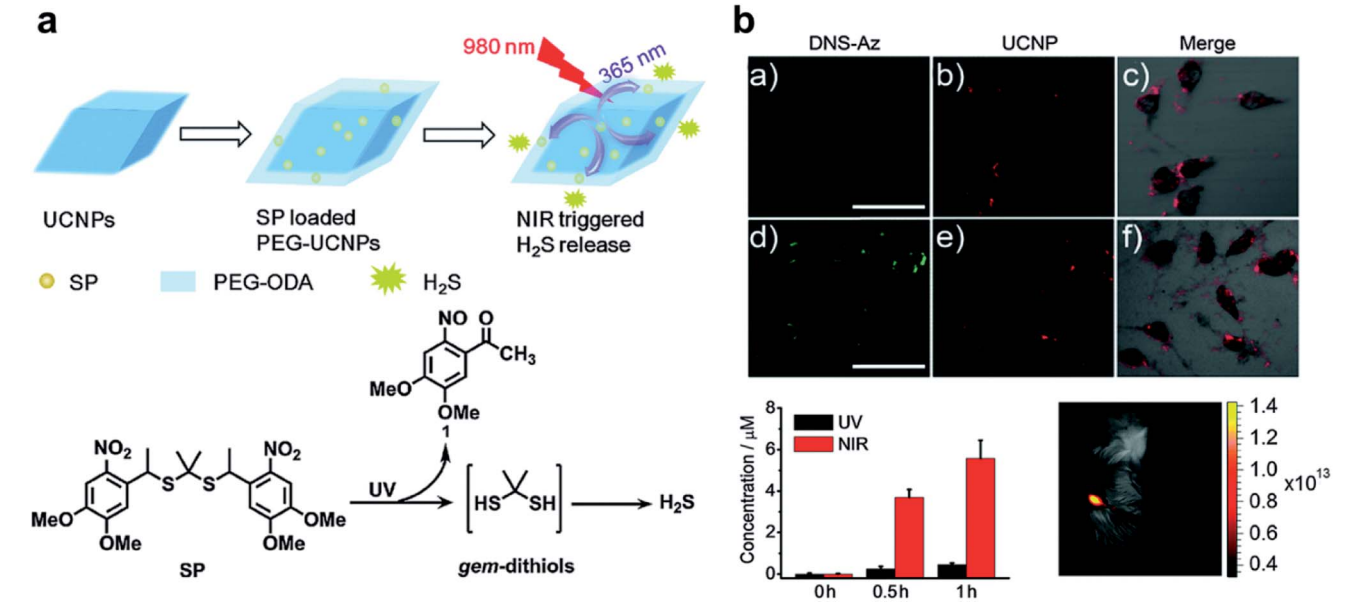

Fig. 6 UCNP-based nanocomposites for H_2S gas therapy. (a) Construction of SP-loaded PEG-UCNPs platform for NIR-triggered H_2S release. (b) H_2S release from SP-loaded PEG-UCNPs with laser irradiation.[38] Adapted from ref. 38 with permission from Royal Society of Chemistry, copyright 2015.

UCNPs through hydrophobic interactions, and SP-loaded UCNPs could trigger H_2S release in a controlled manner through the LRET effect upon 980 nm laser irradiation. In addition, the fluorescence emission of UCNPs could also be used to track the transfer process of H_2S in real-time (Fig. 6b), which was beneficial for regulating the release of H_2S at the specific physiological microenvironment. The UCNP-based gas release strategy provided a new way for the application of H_2S-based gas therapy. Although light stimuli-responsive H_2S nanoplatforms have been developed, the *in vivo* release kinetics of H_2S is still not well known. Furthermore, the biotoxicity of non-specific H_2S release in tissues with high stimuli expression remains a focus of debate. Future drug discovery efforts could utilize the tumor environment to generate specific H_2S donors that are selectively activated in tumor tissues.

3.5 UCNP-based SO_2 gas therapy

High concentrations of SO_2 may disrupt the oxidative stress equilibrium state *via* ROS production, thereby, inducing pathological effects on biomolecules (*e.g.*, lipids, DNA, and proteins). However, efficient SO_2 gas delivery and controlled gas generation are necessary for cancer therapy. A closed-ring isomer of diarylethene, 1-(2,5-dimethylthien-1,1-dioxide-3-yl)-2-(2,5-dimethylthien-3-yl)-hexafluorocyclopentene (DM), showed great thermal stability even at 70 °C, while it rapidly generated SO_2 gas to induce cell death by reverting to the open-ring isomer upon UV irradiation (Fig. 7a).[97] To achieve deeper tissue penetration and lower phototoxicity in SO_2 gas therapy for cancer, UCNP nanocomposites loaded with SO_2 prodrug DM molecules were designed (Fig. 7b).[39] The nanocomposites showed a high drug loading capacity and could photolyze the prodrug to achieve the on-demand release of SO_2. The cytotoxic SO_2 induced the increase of intracellular ROS, which could damage the nuclear DNA, and finally caused apoptosis in cancer cells. The UCNP-DM group showed a significant anti-tumor efficacy, which could be attributed to the high SO_2 generation *via* NIR irradiation. Apart from cancer therapy, such NIR light-triggered UCNP-based SO_2 generation strategy would provide an effective reference for other biomedical applications (*e.g.*, vasorelaxant and anti-bacterial agents).[98,99] Nevertheless, SO_2 gas therapy is still in its infancy, there is still a long way to go before SO_2 gas therapy is ready for clinical use, as potential challenges remain to be well resolved.

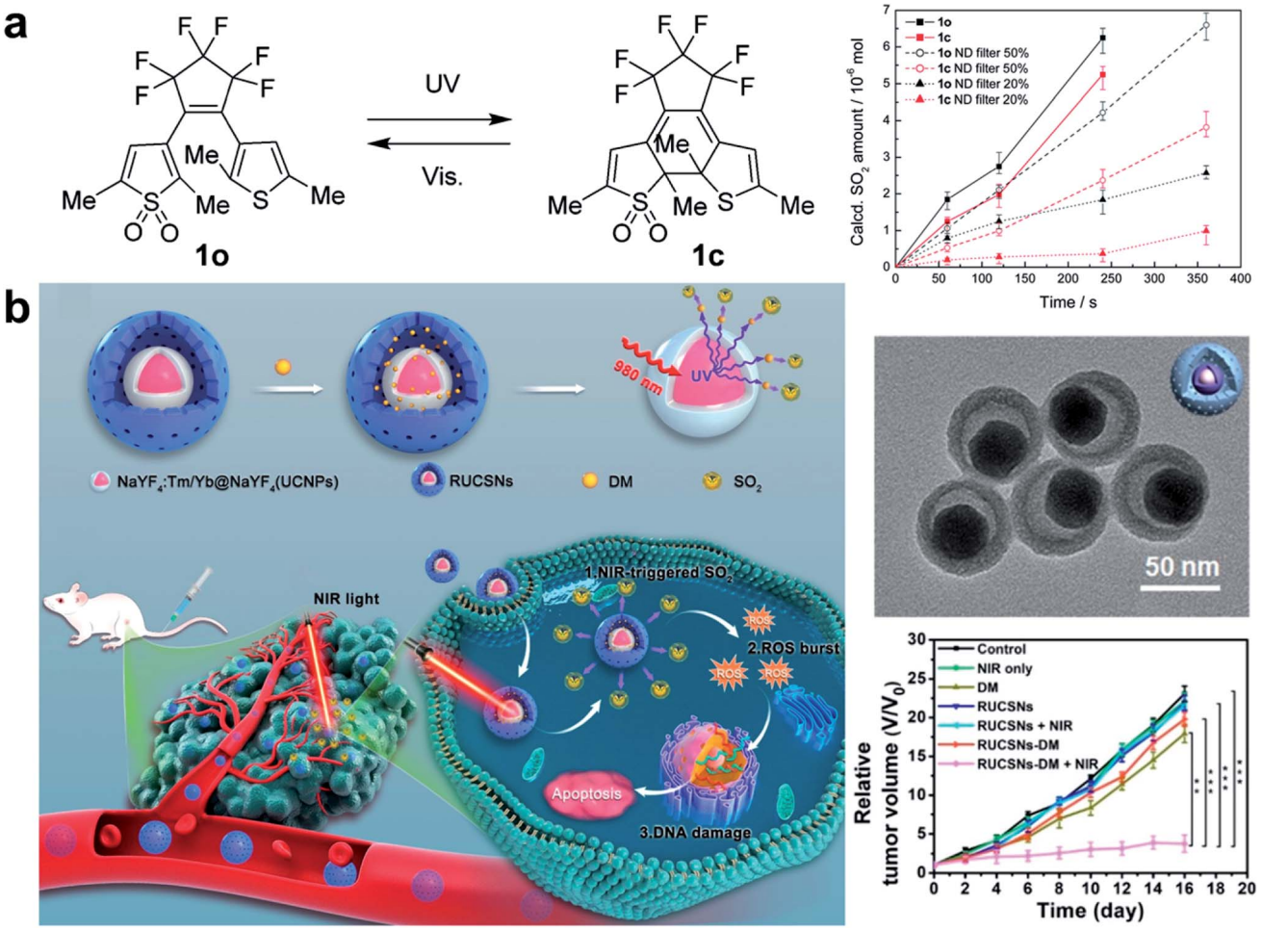

Fig. 7 UCNP-based nanocomposites for SO_2 gas therapy. (a) A diarylethene as the SO_2 gas generator upon UV irradiation.[97] (b) Construction of DM-loaded UCNPs platforms for NIR-triggered SO_2 gas therapy of cancer.[39] Adapted from ref. 97 with permission from Royal Society of Chemistry, copyright 2015; adapted from ref. 39 with permission from American Chemical Society, copyright 2019.

3.6 UCNP-based CO gas therapy

Beyond a certain threshold, high levels of CO may disrupt mitochondrial function, inducing anti-cancer effects. As a CO donor, metal carbonyls (*e.g.*, MnCO, RuCO) that are stabilized by coordination attraction between carbonyls and transition metals, are sensitive to UV/Vis light and are photochemically degraded into CO upon irradiation (Fig. 8a).[37] UCNP-based CO generation nanoplatforms were developed for delivering CO prodrugs and achieving light-responsive CO release (Fig. 8b).[100] NIR light of 808 or 980 nm was absorbed by UCNPs and converted to UV light, thus breaking the Mn–CO bond and releasing CO gas for cancer therapy. It showed dose-dependent cytotoxicity in cancer cells, which meant the importance to construct on-demand gas release therapeutic nanoplatforms. Since a combined therapy was increasingly becoming an effective treatment strategy so far, a lipid-encapsulated nanoplatform that combines chemotherapy with gas therapy was developed by core–shell UCNP-based nanocomposites co-loaded with two therapeutic agents (CO prodrugs and vitamin E analogues).[101] This nanomedicine possessed a tumor-targeting ability and a NIR-triggered CO release ability to inhibit cancer cell growth in a synergistic effect *via* ROS generation and mitochondrial dysfunction (Fig. 8c). Therefore, UCNP-based nanocomposites could be used for controllable CO release in anti-tumor therapy.

However, CO shows adverse biological effects, mainly because of the binding of CO to hemoglobin at higher concentrations *in vivo*. The resulting carboxyhemoglobin reduces the O_2-carrying ability of the blood and leads to tissue hypoxia. *In vitro*, CO inhibits mitochondrial electron transport by irreversibly inhibiting cytochrome c oxidase. The

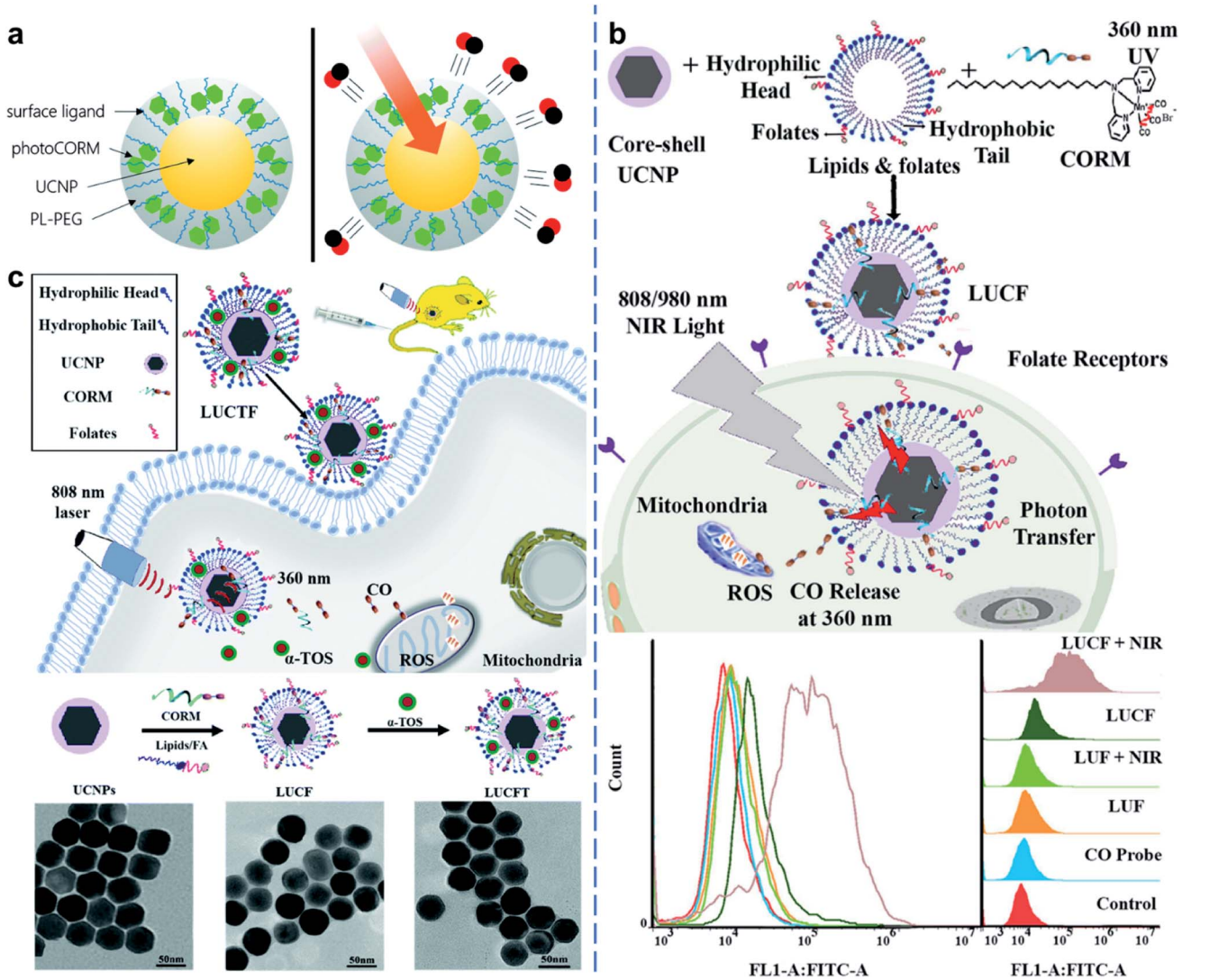

Fig. 8 UCNP-based nanocomposites for CO gas therapy. (a) A photo-activated CO releasing moiety nanocarrier for CO release using NIR light.[37] (b) Lipid-encapsulated UCNPs for NIR-mediated CO release for cancer gas therapy.[100] (c) Vitamin E-facilitated CO pro-drug nanomedicine for efficient light-responsive combination cancer therapy.[101] Adapted from ref. 37 with permission from Royal Society of Chemistry, copyright 2019; adapted from ref. 100 with permission from Elsevier Ltd, copyright 2019; adapted from ref. 101 with permission from Royal Society of Chemistry, copyright 2021.

combination of these harmful effects is considered the central pattern of CO inhalation poisoning. Therefore, it may limit its clinical transformation to a certain extent.

4. Conclusion and prospects

In summary, UCNPs have attracted extensive attention in the past decade due to their unique UCL capability where NIR light with higher tissue penetration depth is converted into higher-energy shorter wavelength UV/Vis light. In this review, we mainly summarized the recent progress of UCNP-based nanocomposites for gas therapy. These gases mainly involved some therapeutic gases that played a vital role in the physiological and pathological processes, such as NO, O_2, H_2, H_2S, SO_2, and CO. UCNPs with unique UCL ability showed great potential to realize the light conversion from long wavelength to short wavelength. This strategy was used to activate the photosensitive gas molecules in cancer therapy, anti-inflammatory therapy, and neuromodulation. However, the UCNP-based nanocomposites for gas therapy is still in its infancy. The long-term toxicity of gas molecules needs to be studied in depth. Although UCNP-based gas therapy strategies had been well developed, there were still some avenues for further development:

(1) Developing novel UCNPs with high luminous efficiency or other excitation wavelengths such as the NIR-II region. Higher luminous efficiency allows lower laser power to achieve the desired biological functions. On the other hand, the NIR-II region shows a higher signal-to-noise ratio due to the reduced light scattering and the decreased water absorption during imaging.[102] UCNP-based gas therapeutic effects and imaging would be greatly improved by NIR-II light excitation.

(2) Further studying the mechanism of gas therapy and developing novel gas donors with more sensitivity to light. Although gas therapy has been developed for many years and has achieved great therapeutic effects in treating various diseases, some therapeutic mechanisms remain unclear. Also, gas release can be achieved upon lower power light irradiation by developing novel and more light-sensitive gas donors, thus, avoiding the potential thermal side effects caused by light irradiation.

(3) Last but not least, bio-applications of UCNP-based gas therapy need further exploration. With the development of nanotechnology and biomedicine, tumor combination therapy has attracted more attention due to its higher efficacy and induced biological effects. The development of the UCNP-based tumor combination therapy (such as gas-immunotherapy) would be a promising therapeutic strategy to prevent tumor metastasis and recurrence. Moreover, since most of the UCNP-based gas therapies reported were centered around cancer treatment, only a few other applications like nerve repair or anti-inflammation. However, various gases have been reported to have many novel functions (*e.g.*, anti-inflammatory, anti-cancer, anti-bacterial, wound healing, immunoregulation, neuromodulation, and the treatment of cardiovascular diseases), but the systematic delivery systems for such gases are still in development.

In summary, it is desirable and necessary to deliver or generate gases based on UCNPs for bio-applications. We hope that this perspective provides insights for further in-depth studies and broad applications of gas therapy.

Data availability

Figures, tables, and detailed information are available from the corresponding author by request.

Author contributions

N. Yang, F. Gong, L. Cheng contributed to the conceptualization, visualization, writing, and editing of the manuscript.

Conflicts of interest

The authors declare no competing financial interest.

Acknowledgements

This article was partially supported by the National Natural Science Foundation of China (U20A20254, 52072253), Collaborative Innovation Center of Suzhou Nano Science and Technology, Suzhou Key Laboratory of Nanotechnology and Biomedicine, a Jiangsu Natural Science Fund for Distinguished Young Scholars (BK20211544), the 111 Project, and Joint International Research Laboratory of Carbon-Based Functional Materials and Devices, and Suzhou Key Laboratory of Nanotechnology and Biomedicine. L. Cheng was supported by the Tang Scholarship of Soochow University.

References

1 G. Chen, H. Qiu, P. N. Prasad and X. Chen, *Chem. Rev.*, 2014, **114**, 5161–5214.
2 Y. Sun, W. Feng, P. Yang, C. Huang and F. Li, *Chem. Soc. Rev.*, 2015, **44**, 1509–1525.
3 S. Wen, J. Zhou, K. Zheng, A. Bednarkiewicz, X. Liu and D. Jin, *Nat. Commun.*, 2018, **9**, 1–12.
4 B. Liu, J. Sun, J. Zhu, B. Li, C. Ma, X. Gu, K. Liu, H. Zhang, F. Wang and J. Su, *Adv. Mater.*, 2020, **32**, 2004460.
5 X. Li, F. Zhang and D. Zhao, *Chem. Soc. Rev.*, 2015, **44**, 1346–1378.
6 G. Liang, H. Wang, H. Shi, H. Wang, M. Zhu, A. Jing, J. Li and G. Li, *J. Nanobiotechnol.*, 2020, **18**, 1–22.
7 L. Cheng, K. Yang, Y. Li, X. Zeng, M. Shao, S.-T. Lee and Z. Liu, *Biomaterials*, 2012, **33**, 2215–2222.
8 L. Cheng, K. Yang, Y. Li, J. Chen, C. Wang, M. Shao, S. T. Lee and Z. Liu, *Angew. Chem., Int. Ed.*, 2011, **123**, 7523–7528.
9 W. Xue, Z. Di, Y. Zhao, A. Zhang and L. Li, *Chin. Chem. Lett.*, 2019, **30**, 899–902.
10 C. Wang, M. Ye, L. Cheng, R. Li, W. Zhu, Z. Shi, C. Fan, J. He, J. Liu and Z. Liu, *Biomaterials*, 2015, **54**, 55–62.
11 S. Fang, C. Wang, J. Xiang, L. Cheng, X. Song, L. Xu, R. Peng and Z. Liu, *Nano Res.*, 2014, **7**, 1327–1336.

12 M. Yin, C. Jing, H. Li, Q. Deng and S. Wang, *J. Nanobiotechnol.*, 2020, **18**, 1–14.
13 C. Wang, L. Cheng and Z. Liu, *Biomaterials*, 2011, **32**, 1110–1120.
14 N. M. Idris, M. K. Gnanasammandhan, J. Zhang, P. C. Ho, R. Mahendran and Y. Zhang, *Nat. Med.*, 2012, **18**, 1580–1585.
15 F. Wang, D. Banerjee, Y. Liu, X. Chen and X. Liu, *Analyst*, 2010, **135**, 1839–1854.
16 L. Cheng, C. Wang and Z. Liu, *Nanoscale*, 2013, **5**, 23–37.
17 Y. Liu, X. Meng and W. Bu, *Coord. Chem. Rev.*, 2019, **379**, 82–98.
18 G. Tian, X. Zhang, Z. Gu and Y. Zhao, *Adv. Mater.*, 2015, **27**, 7692–7712.
19 X. Zhong, X. Wang, G. Zhan, Y. a. Tang, Y. Yao, Z. Dong, L. Hou, H. Zhao, S. Zeng and J. Hu, *Nano Lett.*, 2019, **19**, 8234–8244.
20 L. He, Q. Ni, J. Mu, W. Fan, L. Liu, Z. Wang, L. Li, W. Tang, Y. Liu and Y. Cheng, *J. Am. Chem. Soc.*, 2020, **142**, 6822–6832.
21 L. Chen, S.-F. Zhou, L. Su and J. Song, *ACS Nano*, 2019, **13**, 10887–10917.
22 C. Szabo, *Nat. Rev. Drug Discovery*, 2016, **15**, 185–203.
23 B. Zhao, Y. Wang, X. Yao, D. Chen, M. Fan, Z. Jin and Q. He, *Nat. Commun.*, 2021, **12**, 1–11.
24 Y. Wang, T. Yang and Q. He, *Natl. Sci. Rev.*, 2020, **7**, 1485–1512.
25 L. Yu, P. Hu and Y. Chen, *Adv. Mater.*, 2018, **30**, 1801964.
26 W. Fan, W. Bu, Z. Zhang, B. Shen, H. Zhang, Q. He, D. Ni, Z. Cui, K. Zhao and J. Bu, *Angew. Chem., Int. Ed.*, 2015, **54**, 14026–14030.
27 H. Koo, M. S. Huh, I.-C. Sun, S. H. Yuk, K. Choi, K. Kim and I. C. Kwon, *Acc. Chem. Res.*, 2011, **44**, 1018–1028.
28 W. Fan, B. C. Yung and X. Chen, *Angew. Chem., Int. Ed.*, 2018, **57**, 8383–8394.
29 Y. Jiang, P. Fu, Y. Liu, C. Wang, P. Zhao, X. Chu, X. Jiang, W. Yang, Y. Wu and Y. Wang, *Sci. Adv.*, 2020, **6**, eabc3513.
30 M.-K. Tsang, G. Bai and J. Hao, *Chem. Soc. Rev.*, 2015, **44**, 1585–1607.
31 M. V. DaCosta, S. Doughan, Y. Han and U. J. Krull, *Anal. Chim. Acta*, 2014, **832**, 1–33.
32 R. Lv, D. Yang, P. Yang, J. Xu, F. He, S. Gai, C. Li, Y. Dai, G. Yang and J. Lin, *Chem. Mater.*, 2016, **28**, 4724–4734.
33 J. Xu, F. Zeng, H. Wu, C. Hu, C. Yu and S. Wu, *Small*, 2014, **10**, 3750–3760.
34 P. G. Wang, M. Xian, X. Tang, X. Wu, Z. Wen, T. Cai and A. J. Janczuk, *Chem. Rev.*, 2002, **102**, 1091–1134.
35 K. Hishikawa, H. Nakagawa, T. Furuta, K. Fukuhara, H. Tsumoto, T. Suzuki and N. Miyata, *J. Am. Chem. Soc.*, 2009, **131**, 7488–7489.
36 M. Z. Cabail, P. J. Lace, J. Uselding and A. A. Pacheco, *J. Photochem. Photobiol., A*, 2002, **152**, 109–121.
37 A. E. Pierri, P.-J. Huang, J. V. Garcia, J. G. Stanfill, M. Chui, G. Wu, N. Zheng and P. C. Ford, *Chem. Commun.*, 2015, **51**, 2072–2075.
38 W. Chen, M. Chen, Q. Zang, L. Wang, F. Tang, Y. Han, C. Yang, L. Deng and Y.-N. Liu, *Chem. Commun.*, 2015, **51**, 9193–9196.
39 S. Li, R. Liu, X. Jiang, Y. Qiu, X. Song, G. Huang, N. Fu, L. Lin, J. Song and X. Chen, *ACS Nano*, 2019, **13**, 2103–2113.
40 J. Jia, Z. Wang, M. Zhang, C. Huang, Y. Song, F. Xu, J. Zhang, J. Li, M. He and Y. Li, *Sci. Adv.*, 2020, **6**, eaaz5752.
41 X. Wang, X. Zhong, H. Lei, Y. Geng, Q. Zhao, F. Gong, Z. Yang, Z. Dong, Z. Liu and L. Cheng, *Chem. Mater.*, 2019, **31**, 6174–6186.
42 W.-L. Wan, B. Tian, Y.-J. Lin, C. Korupalli, M.-Y. Lu, Q. Cui, D. Wan, Y. Chang and H.-W. Sung, *Nat. Commun.*, 2020, **11**, 1–9.
43 T. Jia, J. Xu, S. Dong, F. He, C. Zhong, G. Yang, H. Bi, M. Xu, Y. Hu and D. Yang, *Chem. Sci.*, 2019, **10**, 8618–8633.
44 P. T. Burks, J. V. Garcia, R. GonzalezIrias, J. T. Tillman, M. Niu, A. A. Mikhailovsky, J. Zhang, F. Zhang and P. C. Ford, *J. Am. Chem. Soc.*, 2013, **135**, 18145–18152.
45 Y. Yang, Z. Huang and L.-L. Li, *Nanoscale*, 2021, **13**, 444–459.
46 L. Tian, Y. Wang, L. Sun, J. Xu, Y. Chao, K. Yang, S. Wang and Z. Liu, *Matter*, 2019, **1**, 1061–1076.
47 M. A. Evans, P.-J. Huang, Y. Iwamoto, K. N. Ibsen, E. M. Chan, Y. Hitomi, P. C. Ford and S. Mitragotri, *Chem. Sci.*, 2018, **9**, 3729–3741.
48 J. V. Garcia, J. Yang, D. Shen, C. Yao, X. Li, R. Wang, G. D. Stucky, D. Zhao, P. C. Ford and F. Zhang, *Small*, 2012, **8**, 3800–3805.
49 X. Zhang, G. Tian, W. Yin, L. Wang, X. Zheng, L. Yan, J. Li, H. Su, C. Chen and Z. Gu, *Adv. Funct. Mater.*, 2015, **25**, 3049–3056.
50 J. Zhao, Y. Hu, S. wei Lin, U. Resch-Genger, R. Zhang, J. Wen, X. Kong, A. Qin and J. Ou, *J. Mater. Chem. B*, 2020, **8**, 6481–6489.
51 S. Liu, W. Li, S. Dong, F. Zhang, Y. Dong, B. Tian, F. He, S. Gai and P. Yang, *Nanoscale*, 2020, **12**, 24146–24161.
52 S. Li, X. Song, W. Zhu, Y. Chen, R. Zhu, L. Wang, X. Chen, J. Song and H. Yang, *ACS Appl. Mater. Interfaces*, 2020, **12**, 30066–30076.
53 X. Chu, X. Jiang, Y. Liu, S. Zhai, Y. Jiang, Y. Chen, J. Wu, Y. Wang, Y. Wu and X. Tao, *Adv. Funct. Mater.*, 2021, **31**, 2008507.
54 J. Sun, Y. Fan, W. Ye, L. Tian, S. Niu, W. Ming, J. Zhao and L. Ren, *Chem. Eng. J.*, 2021, **417**, 128049.
55 K. Dong, E. Ju, N. Gao, Z. Wang, J. Ren and X. Qu, *Chem. Commun.*, 2016, **52**, 5312–5315.
56 H. Liang, Z. Li, Z. Ren, Q. Jia, L. Guo, S. Li, H. Zhang, S. Hu, D. Zhu and D. Shen, *Nano Res.*, 2020, **13**, 2197–2202.
57 J. Ye, J. Jiang, Z. Zhou, Z. Weng, Y. Xu, L. Liu, W. Zhang, Y. Yang, J. Luo and X. Wang, *ACS Nano*, 2021, **15**, 13692–13702.
58 F. B. Wagner, J.-B. Mignardot, C. G. Le Goff-Mignardot, R. Demesmaeker, S. Komi, M. Capogrosso, A. Rowald, I. Seáñez, M. Caban and E. Pirondini, *Nature*, 2018, **563**, 65–71.

59 J. Koffler, W. Zhu, X. Qu, O. Platoshyn, J. N. Dulin, J. Brock, L. Graham, P. Lu, J. Sakamoto and M. Marsala, *Nat. Med.*, 2019, **25**, 263–269.
60 G. Yang, S. Z. F. Phua, W. Q. Lim, R. Zhang, L. Feng, G. Liu, H. Wu, A. K. Bindra, D. Jana and Z. Liu, *Adv. Mater.*, 2019, **31**, 1901513.
61 X. Liu, Y. Hao, R. Popovtzer, L. Feng and Z. Liu, *Adv. Healthcare Mater.*, 2021, **10**, 2001167.
62 M. Gao, C. Liang, X. Song, Q. Chen, Q. Jin, C. Wang and Z. Liu, *Adv. Mater.*, 2017, **29**, 1701429.
63 G. Song, C. Ji, C. Liang, X. Song, X. Yi, Z. Dong, K. Yang and Z. Liu, *Biomaterials*, 2017, **112**, 257–263.
64 C. Wang, C. Liang, Y. Hao, Z. Dong, Y. Zhu, Q. Li, Z. Liu, L. Feng and M. Chen, *Chem. Eng. J.*, 2021, **414**, 128731.
65 J. Wang, X. Wang, S.-Y. Lu, J. Hu, W. Zhang, L. Xu, D. Gu, W. Yang, W. Tang and F. Liu, *Biomaterials*, 2019, **223**, 119465.
66 Z. Yang, Q. Chen, J. Chen, Z. Dong, R. Zhang, J. Liu and Z. Liu, *Small*, 2018, **14**, 1803262.
67 Y. Yang, W. Zhu, L. Feng, Y. Chao, X. Yi, Z. Dong, K. Yang, W. Tan, Z. Liu and M. Chen, *Nano Lett.*, 2018, **18**, 6867–6875.
68 F. Gong, L. Cheng, N. Yang, Y. Gong, Y. Ni, S. Bai, X. Wang, M. Chen, Q. Chen and Z. Liu, *Nat. Commun.*, 2020, **11**, 1–11.
69 X. Wang, X. Wang, Q. Yue, H. Xu, X. Zhong, L. Sun, G. Li, Y. Gong, N. Yang and Z. Wang, *Nano Today*, 2021, **39**, 101170.
70 N. Yang, F. Gong, Y. Zhou, Y. Hao, Z. Dong, H. Lei, L. Zhong, X. Yang, X. Wang and Y. Zhao, *Biomaterials*, 2021, 121125.
71 N. Yang, F. Gong, L. Cheng, H. Lei, W. Li, Z. Sun, C. Ni, Z. Wang and Z. Liu, *Natl. Sci. Rev.*, 2021, **8**, nwaa122.
72 W. Fan, W. Bu, B. Shen, Q. He, Z. Cui, Y. Liu, X. Zheng, K. Zhao and J. Shi, *Adv. Mater.*, 2015, **27**, 4155–4161.
73 F. Gong, N. Yang, X. Wang, Q. Zhao, Q. Chen, Z. Liu and L. Cheng, *Nano Today*, 2020, **32**, 100851.
74 J. Liu, Q. Chen, L. Feng and Z. Liu, *Nano Today*, 2018, **21**, 55–73.
75 R. Cao, W. Sun, Z. Zhang, X. Li, J. Du, J. Fan and X. Peng, *Chin. Chem. Lett.*, 2020, **31**, 3127–3130.
76 G. Yang, L. Xu, Y. Chao, J. Xu, X. Sun, Y. Wu, R. Peng and Z. Liu, *Nat. Commun.*, 2017, **8**, 1–13.
77 Q. Chen, L. Feng, J. Liu, W. Zhu, Z. Dong, Y. Wu and Z. Liu, *Adv. Mater.*, 2016, **28**, 7129–7136.
78 T. Gu, L. Cheng, F. Gong, J. Xu, X. Li, G. Han and Z. Liu, *ACS Appl. Mater. Interfaces*, 2018, **10**, 15494–15503.
79 X. Wu, P. Yan, Z. Ren, Y. Wang, X. Cai, X. Li, R. Deng and G. Han, *ACS Appl. Mater. Interfaces*, 2018, **11**, 385–393.
80 D. Ni, H. Wei, W. Chen, Q. Bao, Z. T. Rosenkrans, T. E. Barnhart, C. A. Ferreira, Y. Wang, H. Yao and T. Sun, *Adv. Mater.*, 2019, **31**, 1902956.
81 Q. Weng, H. Sun, C. Fang, F. Xia, H. Liao, J. Lee, J. Wang, A. Xie, J. Ren and X. Guo, *Nat. Commun.*, 2021, **12**, 1–14.
82 F. Li, Y. Qiu, F. Xia, H. Sun, H. Liao, A. Xie, J. Lee, P. Lin, M. Wei and Y. Shao, *Nano Today*, 2020, **35**, 100925.
83 C. Yao, W. Wang, P. Wang, M. Zhao, X. Li and F. Zhang, *Adv. Mater.*, 2018, **30**, 1704833.
84 Y. Zhang, H. Liu, X. Dai, H. Li, X. Zhou, S. Chen, J. Zhang, X.-J. Liang and Z. Li, *Nano Res.*, 2021, **14**, 667–673.
85 H. Zhao, J. Huang, Y. Li, X. Lv, H. Zhou, H. Wang, Y. Xu, C. Wang, J. Wang and Z. Liu, *Biomaterials*, 2020, **258**, 120286.
86 H. Chen, Y. Cheng, J. Tian, P. Yang, X. Zhang, Y. Chen, Y. Hu and J. Wu, *Sci. Adv.*, 2020, **6**, eaba4311.
87 H. Thangarajah, D. Yao, E. I. Chang, Y. Shi, L. Jazayeri, I. N. Vial, R. D. Galiano, X.-L. Du, R. Grogan and M. G. Galvez, *Proc. Natl. Acad. Sci.*, 2009, **106**, 13505–13510.
88 M. Dole, F. R. Wilson and W. P. Fife, *Science*, 1975, **190**, 152–154.
89 R. Sun, X. Liu, G. Li, H. Wang, Y. Luo, G. Huang, X. Wang, G. Zeng, Z. Liu and S. Wu, *ACS Nano*, 2020, **14**, 8135–8148.
90 W. L. Wan, Y. J. Lin, P. C. Shih, Y. R. Bow, Q. Cui, Y. Chang, W. T. Chia and H. W. Sung, *Angew. Chem., Int. Ed.*, 2018, **130**, 10023–10027.
91 P. Zhao, Z. Jin, Q. Chen, T. Yang, D. Chen, J. Meng, X. Lu, Z. Gu and Q. He, *Nat. Commun.*, 2018, **9**, 1–12.
92 J.-B. Chen, X.-F. Kong, F. Mu, T.-Y. Lu, Y.-Y. Lu and K.-C. Xu, *Med. Gas Res.*, 2020, **10**, 75.
93 D. Du, L. Zhao, M. Shen, M. Noda, S. Qin, J. Long, X. Sun and J. Liu, *Tradit. Med. Mod. Med.*, 2021, 1–9.
94 Y. Wu, M. Yuan, J. Song, X. Chen and H. Yang, *ACS Nano*, 2019, **13**, 8505–8511.
95 J. Chen, S. Lin, D. Zhao, L. Guan, Y. Hu, Y. Wang, K. Lin and Y. Zhu, *Adv. Funct. Mater.*, 2021, **31**, 2006853.
96 B. Liu, S. Liang, Z. Wang, Q. Sun, F. He, S. Gai, P. Yang, Z. Cheng and J. Lin, *Adv. Mater.*, 2021, 2101223.
97 R. Kodama, K. Sumaru, K. Morishita, T. Kanamori, K. Hyodo, T. Kamitanaka, M. Morimoto, S. Yokojima, S. Nakamura and K. Uchida, *Chem. Commun.*, 2015, **51**, 1736–1738.
98 Z. Meng, J. Li, Q. Zhang, W. Bai, Z. Yang, Y. Zhao and F. Wang, *Inhalation Toxicol.*, 2009, **21**, 1223–1228.
99 S. R. Malwal, D. Sriram, P. Yogeeswari, V. B. Konkimalla and H. Chakrapani, *J. Med. Chem.*, 2012, **55**, 553–557.
100 Y. Opoku-Damoah, R. Zhang, H. T. Ta, D. A. Jose, R. Sakla and Z. P. Xu, *Eur. J. Pharm. Biopharm.*, 2021, **158**, 211–221.
101 Y. Opoku-Damoah, R. Zhang, H. T. Ta and Z. P. Xu, *Biomater. Sci.*, 2021, **9**, 6086–6097.
102 S. Liu, Y. Li, R. T. Kwok, J. W. Lam and B. Z. Tang, *Chem. Sci.*, 2021, **12**, 3427–3436.